

## Competing local exchange mechanisms: a validity test of a simple scaling hypothesis

This article has been downloaded from IOPscience. Please scroll down to see the full text article.

1992 J. Phys.: Condens. Matter 4 7229

(<http://iopscience.iop.org/0953-8984/4/35/008>)

View [the table of contents for this issue](#), or go to the [journal homepage](#) for more

Download details:

IP Address: 171.66.16.96

The article was downloaded on 11/05/2010 at 00:28

Please note that [terms and conditions apply](#).

## Competing local exchange mechanisms: a validity test of a simple scaling hypothesis

F B Anders†, Qi Qin‡ and N Grewe†

† Institut für Festkörperphysik, Technische Hochschule, D-6100 Darmstadt, Federal Republic of Germany

‡ Institut für Theoretische Physik, Universität D-2800 Bremen, Federal Republic of Germany

Received 22 April 1992, in final form 2 June 1992

**Abstract.** The interplay of a direct ferromagnetic exchange interaction  $I > 0$  between local and band states and an indirect antiferromagnetic exchange  $-J < 0$  via hybridization  $V$  is studied using an expanded version of the Anderson impurity model in the highly correlated regime. A simple scaling idea is put forward for the dependence of the free energy, one-particle spectra,  $T$ -matrix and susceptibility on the size of hybridization and direct exchange. It describes the many-body regime  $J \gg I$  in terms of a universal picture as well as the crossover near  $J \approx I$  to the trivial regime  $J \ll I$ , the latter being characterized by an effective elastic one-particle scattering problem. These physical arguments are supported by extensive numerical calculations in the framework of perturbation theory with respect to  $I$  and  $V$ . It is also indicated how  $I$  may be included into new post-NCA theories of the Kondo effect.

### 1. Introduction

Recently, Keller and co-workers [1] have proposed extending existing many-body theories for the Anderson model in order to incorporate additional Coulomb-matrix elements. Indeed, it seems very important to improve on simple effective models, which neglect most interaction processes and treat others in a mean field fashion only, in order to make better contact to, e.g., bandstructure calculations. Also, a more general applicability to a wider span of materials and specific parameter configurations is desirable, which would allow for a more consistent description of different correlation phenomena in one theoretical frame. In view of the variety of possible terms in the Hamiltonian, for, e.g., transition metal compounds, mixing of one-particle states due to non-orthogonality and different local and non-local Coulomb-matrix elements, information regarding their particular role in the basic physical picture and possible allowed simplifications is certainly useful. In their studies of Coulomb interactions between local and band electrons Keller *et al* have demonstrated the disappearance of the Kondo effect with increasing direct exchange  $I$ . They have also, using different kinds of many-body techniques, i.e. the slave-boson approach [1] and direct perturbation theory [2], put forward questions about the role of residual many-body correlations of magnetic or charge-transfer type. We will try to shed some light on this issue by demonstrating for the case of additional exchange interactions a rather

strict scaling behaviour of thermodynamic and dynamic quantities, in which only one effective parameter

$$\Delta^* \equiv \Delta(1 - I/J) = \pi \mathcal{N}_F (V^2 - I|\Delta E|)$$

determines the size of physical effects in the whole span between the regimes  $I < J$ , characterized by Kondo effect and corresponding many-body correlations, and  $I > J$ , where only 'trivial' one-particle scattering prevails. Here  $V$  is a hybridization-matrix element,  $\mathcal{N}_F$  the DOS at the Fermi level  $\epsilon_F = 0$ ,  $\Delta E = E_1 - E_0 < 0$  the unrenormalized energy difference between the relevant ionic levels (assuming infinite ionic Coulomb repulsion and residual degeneracy  $n = 2$ ),  $-J = V^2/\Delta E < 0$  the indirect exchange coupling [3] and  $\Delta = \pi V^2 \mathcal{N}_F$  the unrenormalized Anderson width. An intuitive justification is guided by the physics of the Schrieffer-Wolff transformation [4], whereas a comparison with full NCA calculations furnishes a quantitative basis of this picture. We will also indicate how  $I$  can be fitted naturally into an advanced post NCA theory which is currently being developed.

A Hamiltonian for the problem studied here reads

$$H = \sum_{k,m} \epsilon_k c_{km}^\dagger c_{km} + \sum_m \Delta E_m X_{mm} + \frac{1}{\sqrt{N}} \sum_{k,m} [V_{km} X_{m0} c_{km} + \text{HC}] - \frac{1}{N} \sum_{\substack{k,k' \\ m,m'}} I_{kk'}^{m,m'} X_{m,m'} c_{k'm'}^\dagger c_{km} \quad (1)$$

where  $E_0 = 0$ ,  $X_{MM'}$  are Hubbard's ionic operators for transferring from state  $M$  to state  $M'$ , where  $M = (n_{\text{loc}} =) 0$  or  $(n_{\text{loc}} = 1, j_z =) m$ . As a consequence of an assumed very large electron repulsion,  $U_{\text{loc}}$ , in the local orbital the state  $n_{\text{loc}} = 2$  is omitted. The processes encountered in direct perturbation theory can be visualized along a local time axis containing a wavy or broken line for the occupied or empty local state, vertices in the form of full dots or full squares for the last two terms in equation (1), i.e. the perturbations  $V$  and  $I$ , and straight band electron lines attached to them from the right. The exact transcription into analytical contributions is intuitive, straightforward and well documented in earlier work [5, 8]. Hybridization of an electron from the local state into the band will be followed by an immediate reabsorption of a band electron, possibly with different spin, if the local excitation energy  $-\Delta E$  is much larger than the one-particle level width  $\Delta$  acquired by such a hybridization processes. In this extreme Kondo limit the dynamics is thus effectively described by pairs of vertices without retardation, i.e. an effective potential scattering and an indirect exchange term. The latter antiferromagnetic interaction with a strength  $J = V^2/(z - \Delta E) \approx V^2/|\Delta E| (z \approx 0)$  causes the Kondo effect and will be considered here together with the direct ferromagnetic exchange  $I > 0$ . It is thus to be expected that a total exchange coupling 'constant'

$$I_{kk'}^{*m,m'} = I_{kk'}^{m,m'} - \frac{V_{km} V_{k'm'}}{z - \Delta E} \Big|_{|z| \ll |\Delta E|} \approx I_{kk'}^{m,m'} - \frac{V_{km} V_{k'm'}}{|\Delta E|} \quad (2)$$

will be relevant for the dynamics of the magnetic degrees of freedom. On the other hand, the one-particle scattering is also different in the presence of  $I$ . It will be

shown below that in the absence of spin-flip scattering an effective model with a local  $T$ -matrix  $(1/N)(V^2 G_{\text{loc}}^{(0)}(z) - I)$  arises in leading order. When the unperturbed local Green function  $G_{\text{loc}}^{(0)}(z) = 1/(z - \Delta E)$  is again taken near the Fermi level, i.e.  $z \approx 0$ , an effective hybridization intensity or Anderson width results:

$$\Delta \equiv \pi \langle V^2 \rangle \mathcal{N}_F \rightarrow \pi \mathcal{N}_F (\langle V^2 \rangle - \langle I | \Delta E | \rangle) \equiv \Delta^* \quad (3)$$

(the brackets indicate an averaging over quantum numbers  $m$  and  $k$ ) which is relevant for the one-particle properties near  $\epsilon_F$ . From this discussion we draw the following conclusions.

(i) The physics of the Hamiltonian (1), in the regime where direct and indirect exchange couplings are smaller than the valence excitation energy  $\Delta E$ , is to a good approximation equivalent to that of an  $s$ - $d$  model with an appropriately rescaled interaction term. In particular, the two qualitatively different cases of ferro- and antiferromagnetic interaction fit into this scaling picture as follows. (a) In the Kondo regime of model (1), i.e.  $\Delta \ll |\Delta E| \ll \mathcal{N}_F^{-1} \approx 2W$  bandwidth (the Coulomb repulsion  $U_{\text{loc}}$  being infinite) and  $I^* < 0$ , the low-temperature state will be ruled by many-body effects with a new energy scale

$$k_B T_K^* = W \left( \frac{\Delta^*}{\pi W} \right)^{1/n} \exp \left[ - \frac{\pi |\Delta E|}{n \Delta^*} \right] \quad n = \#m. \quad (4)$$

Universal behaviour [6, 27] related to this scale is expected [7]. (b) In the ferromagnetic regime of model (1), i.e.  $0 < \Delta \ll |\Delta E| \ll \mathcal{N}_F^{-1}$  and  $I^* > 0$ , spin-flip processes are essentially frozen out, and only one-particle scattering is left. It may be attributed to an effective longitudinal exchange coupling  $I^* = I - V^2/(z - \Delta E)$  which becomes  $I^* = -\Delta^*/(\pi \mathcal{N}_F |\Delta E|) > 0$  for  $z$  near  $\epsilon_F = 0$ .

(ii) Possible deviations from this picture have to be attributed to the effect of charge fluctuations, which spoil the applicability of the Schrieffer–Wolff transformation.

## 2. Theory

The scaling picture proposed above, which contains only one effective parameter  $\Delta^*$ , will be tested and verified on the basis of direct perturbation theory [8], which has proven to be a valuable and essentially correct tool in problems with strong local electron correlations like the Kondo impurity [9], the heavy-fermion problem [10] or the metal–insulator transition as described by the Hubbard model [11]. The prototypical theory is the non-crossing approximation (NCA) for the Anderson model in the Kondo regime, which produces as in the  $x$ -ray problem [19–21] a proper threshold behaviour for the ionic resolvents

$$\mathcal{P}_M(z) = \langle M | \left\langle \frac{1}{z - H} \right\rangle_c | M \rangle = [z - E_M - \Sigma_M(z)]^{-1}$$

where  $\langle \dots \rangle_c$  is a partial trace on band states, the exact (Wilson) dynamic energy scale  $T_K = T_K^*(\Delta^* \rightarrow \Delta)$ , see equation (4), and the well known Abrikosov–Suhl (AS) resonance near the Fermi level. A few years ago it was extended to finite values of the

local Coulomb repulsion  $U_{loc}$ , and again good agreement with physical expectations and results known from other theories was found [12]. Certain shortcomings for small  $n = \#m$ , in particular  $n = 2$ , which concern analyticity at the Fermi level and small deviations from the DOS sum rule [13, 14] can be controlled [15], but have nevertheless caused a need for improvement, in particular in connection with the (i.e. Kondo-) lattice problems where the correct Fermi-liquid behaviour is essential, i.e. in transport calculations.

The most recent state of direct perturbation theory [16] is summarized in the following graphical representation of contributions to the ionic self-energies  $\Sigma_M(z)$ :

$$\begin{aligned}
 \Sigma_0(z) : &= \text{diagram 1} + \text{diagram 2} + \text{diagram 3} + \text{diagram 4} \\
 \Sigma_m(z) : &= \text{diagram 5} + \text{diagram 6} + 2 \times \text{diagram 7} + \text{diagram 8} \\
 &+ \text{diagram 9} + \text{diagram 10}
 \end{aligned}
 \tag{5}$$

The diagrams in equation (5) represent various self-energy contributions. Diagram 1 is a simple loop with two vertices. Diagrams 2-4 show more complex interactions involving multiple sites and internal loops. Diagrams 5-10 show contributions to the self-energy of a specific site  $m$ , including diagrams with dashed lines and multiple internal interactions.

with

$$\text{diagram 11} = \text{diagram 12} + \text{diagram 13}
 \tag{6}$$

Diagram 11 shows a vertex correction where a shaded square is inserted into a loop. Diagram 12 shows the same vertex correction with a different internal structure. Diagram 13 shows a more complex vertex correction involving multiple sites and internal loops.

$$\begin{array}{c}
 \begin{array}{ccc}
 \begin{array}{c} m \\ \diagup \\ \square \\ \diagdown \\ m' \end{array} & \begin{array}{c} km \\ \diagup \\ \square \\ \diagdown \\ km' \end{array} \\
 \end{array} & = & \begin{array}{c} m \\ \diagup \\ \square \\ \diagdown \\ m' \end{array} & \begin{array}{c} km \\ \diagup \\ \square \\ \diagdown \\ km' \end{array} & + & \begin{array}{c} m \\ \diagup \\ \bullet \\ \vdots \\ \bullet \\ \diagdown \\ m' \end{array} & \begin{array}{c} km \\ \diagup \\ \bullet \\ \vdots \\ \bullet \\ \diagdown \\ km' \end{array} \\
 \end{array} \tag{7}$$

$$\begin{array}{c}
 \begin{array}{ccc}
 \begin{array}{c} m \\ \diagup \\ \circ \\ \diagdown \\ m \end{array} & \begin{array}{c} km' \\ \diagup \\ \circ \\ \diagdown \\ km' \end{array} \\
 \end{array} & := & \begin{array}{c} m \\ \diagup \\ \square \\ \diagdown \\ m' \end{array} & \begin{array}{c} km' \\ \diagup \\ \text{---} \\ \diagdown \\ \square \\ \diagdown \\ m \end{array} & \begin{array}{c} km \\ \diagup \\ \square \\ \diagdown \\ km' \end{array} \\
 \end{array} \tag{8}$$

$$\begin{array}{c}
 \begin{array}{ccc}
 \begin{array}{c} m \\ \diagup \\ \bullet \\ \diagdown \\ m \end{array} & \begin{array}{c} km' \\ \diagup \\ \bullet \\ \diagdown \\ km' \end{array} \\
 \end{array} & = & \begin{array}{c} m \\ \diagup \\ \circ \\ \diagdown \\ m \end{array} & \begin{array}{c} km' \\ \diagup \\ \circ \\ \diagdown \\ km' \end{array} & + & \begin{array}{c} m \\ \diagup \\ \bullet \\ \text{---} \\ \bullet \\ \diagdown \\ m \end{array} & \begin{array}{c} km' \\ \diagup \\ \bullet \\ \text{---} \\ \bullet \\ \diagdown \\ km' \end{array} \\
 \end{array} \tag{9}$$

These coupled equations, formulated in terms of skeletons in the diagrammatic language introduced above, are selfconsistent like the NCA in the sense of Baym [17], but go considerably further. In the systematics of the  $1/n$ -expansion scheme they consistently contain all skeleton diagrams up to order  $1/n^2$ . Furthermore, they incorporate the direct ferromagnetic exchange  $I$  in a natural way. Each vertex  $I$  corresponds to two orders of the hybridization vertex and is in fact treated jointly according to equation (2) in the classification of higher skeletons with crossing band electron lines. This system of integral equations exhibits a very interesting and new threshold behaviour [18] and preliminary numerical studies indeed indicate an improvement over the NCA in the way outlined above. We take this as an additional clue to the applicability of effective theories for the extended model with two different exchange mechanisms, but will for the purpose of a detailed comparison restrict ourselves at present to a kind of effective NCA theory [2]. This much simpler approximation avoids the numerical efforts connected with threefold integrations over band energies—the system (5) can at most be written in a way which needs (only) threefold integrations, compared e.g. to twofold integrations which have been mastered in the NCA-version at finite  $U_{loc}$ . Thus the first two diagrams for  $\Sigma_0(z)$  and the first five for  $\Sigma_m(z)$  are retained here. The corresponding analytical expressions yield the following system to be evaluated:

$$\begin{aligned}
 \Sigma_0(z) &= |V^2| \mathcal{X}(z) / (1 - I \mathcal{X}(z)) \\
 \Sigma_m(z) &= \frac{1}{N} \sum_k \frac{f(-\epsilon_k)}{1 - I \mathcal{X}(z - \epsilon_k)} \left[ I + |V|^2 \frac{\mathcal{P}_0(z - \epsilon_k)}{1 - I \mathcal{X}(z - \epsilon_k)} \right] \\
 \mathcal{X}(z) &= \frac{1}{N} \sum_{km} f(\epsilon_k) \mathcal{P}_m(z + \epsilon_k).
 \end{aligned} \tag{10}$$

For simplicity, also, any dependence of the vertices  $V$  and  $I$  on quantum numbers  $k$  and  $m$  will be neglected. After these self-energies have been determined by numerical iteration, the ionic resolvents are known, too, and partition function  $\mathcal{Z}_{\text{loc}}$  and the local Green function (GF) [8]

$$\begin{aligned} \langle\langle X_{0m}|X_{m0}\rangle\rangle(z) &= \frac{1}{\mathcal{Z}_{\text{loc}}} \int_C \frac{dz'}{2\pi i} e^{-\beta z'} \mathcal{P}_0(z') \mathcal{P}_m(z+z') \\ \mathcal{Z}_{\text{loc}} &= \sum_{M=0,m} \int_C \frac{dz}{2\pi i} e^{-\beta z} \mathcal{P}_M(z) \end{aligned} \quad (11)$$

can be calculated, which also furnishes the spectral density

$$\mathcal{N}^{\text{loc}}(\omega) = -(1/\pi) \text{Im} \langle\langle X_{0m}|X_{m0}\rangle\rangle(\omega + i\delta) \quad (12)$$

of local one-particle excitations. Fermi liquid theory [13, 14] predicts a value somewhat smaller than  $1/\pi\Delta$  for the Kondo problem at the Fermi level at  $T = 0$ , thus pointing toward scaling with  $V^2 \sim \Delta$ ; see equation (10) in reference [14]. The free energy  $F_{\text{loc}} = -(1/\beta) \ln \mathcal{Z}_{\text{loc}}$ , the spectrum (12) as well as the local susceptibility

$$\chi(\omega) = \frac{1}{\mathcal{Z}_{\text{loc}}} \int_C \frac{dz'}{2\pi i} e^{-\beta z'} \mathcal{P}_m(z') \mathcal{P}_m(z'+\omega) \quad (13)$$

are well studied and understood, e.g. for the Kondo problem and will help to check our scaling hypothesis. (Note that the magnetic susceptibility is quoted in its natural units  $(nJ(J+1)g^2\mu_B^2)/3$  [19].)

A particular role is played by the scattering matrix for band electrons (short:  $T$ -matrix) in so far as it incorporates the action of the local degrees of freedom even when they do not appear explicitly as local electrons, e.g. in the form of a direct exchange interaction  $I$  only, as in the s-d model for the Kondo problem. For the Anderson model on the other hand, given by equation (1) with  $I = 0$ , it is easy to show by, e.g., the equation of motion method that the  $T$ -matrix, formally defined by

$$\langle\langle c_{km}|c_{k'm'}^\dagger\rangle\rangle(z) = G_{km}^{(0)}(z)\delta_{kk'}\delta_{mm'} + G_{km}^{(0)}(z)T_{kk'}^{mm'}(z)G_{k'm'}^{(0)}(z) \quad (14)$$

where  $G_{km}^{(0)}(z) = (z - \epsilon_k)^{-1}$  is the unperturbed band GF, is simply proportional to the local GF

$$T_{kk'}^{mm'}(z) = \delta_{mm'}(1/N)V_{km}\langle\langle X_{0m}|X_{m0}\rangle\rangle(z)V_{k'm}^*. \quad (15)$$

It thus contains the same spectral information about the original resonance near  $\Delta E$  and about the AS resonance near the Fermi level. By taking the limit  $\Delta E \rightarrow -\infty$  at constant  $V$  the Anderson model can be mapped onto an s-d model with an antiferromagnetic exchange  $-J$  [4], which is also a special case of equation (1) with  $V = 0$  and  $I < 0$ . The  $T$ -matrix should always reflect the many-body effects near  $\epsilon_F$  in the following way. A very narrow spike remains near  $\epsilon_F$  as representative in weight of the exponentially small  $T_K \sim e^{-1/(nJN_F)}$  with peak-heights of  $(\pi N_F)^{-1}$  independent of  $I$  at  $T = 0$ , which finally becomes a point of discontinuity when  $I \equiv J$  reaches zero and  $T_K = 0$ . In the present general context the  $T$ -matrix

$$T_{kk'}^{mm'}(z) = \frac{\delta_{mm'}}{N} \frac{1}{\mathcal{Z}_{\text{loc}}} \int_C \frac{dz'}{2\pi i} e^{-\beta z'} \mathcal{P}_m(z+z') \left[ \frac{I}{1 - I\mathcal{X}(z')} + \frac{|V|^2 \mathcal{P}_0(z')}{[1 - I\mathcal{X}(z')]^2} \right] \quad (16)$$

is  $k$ -independent and can be obtained diagrammatically in NCA by cutting in all skeleton contributions to  $\Sigma_m(z)$ , see equation (10), the band electron line running into the uppermost vertex point and removing the corresponding external band GF. For completeness, we also give the full set of contributions to  $T_{kk'}^{mm'}(z) = (\delta_{mm'}/N)T_{kk'}^m(z)$  consistently to order  $1/n^2$  including the non-crossing skeletons from equation (5):

$$T_{kk'}^{mm'}(z) = \dots + \dots + 2 \dots + \dots + \dots + \dots + \dots \tag{17}$$

Equation (16) completes the list of analytical results in the frame of a generalized NCA which will be evaluated numerically.

We will also apply the formalism outlined above to the ‘ferromagnetic regime’  $I^* > 0$ , where many-body correlations should not be present in the impurity model (1). Due to the effective ferromagnetic exchange, spin compensation cannot occur and spin-flip scattering is suppressed. As for the resonant level model ( $\#m = n = 1$ ) [9] the NCA can also be expected to furnish a reasonable description of this trivial case. One expects a mapping of Hamiltonian (1) onto an effective ferromagnetic s-d model

$$H = \sum_{k,m} \epsilon_k c_{km}^\dagger c_{km} - \frac{4}{\hbar^2} \frac{1}{N} \sum_{kk'} [\tilde{I}_\parallel S_z^{\text{loc}} + \frac{1}{2} \tilde{I}_\perp (S_+^{\text{loc}} s_-^c + S_-^{\text{loc}} s_+^c)] \tag{18}$$

where  $\tilde{I}_\parallel = \tilde{I}_\perp = I^* \langle X_{mm} \rangle > 0$ ,  $S^{\text{loc}}$  and  $s^c$  are the spin operators of local and band electrons respectively, and pure spin degeneracy  $\#m = n = 2$  is assumed for simplicity. The longitudinal term  $\sim \tilde{I}_\parallel$  in (18) now works as an attractive potential for the equal spin species of electrons in the band, which effectively freezes out spin-flip scattering contained in the transversal terms  $\sim \tilde{I}_\perp$ . The problem thus scales to a trivial fixed point [22] with  $\tilde{I}_\perp = 0$ . It is easy to apply the equation of motion technique to the original model (1), when contributions violating conservation of the quantum number  $m$  can be neglected. The resulting  $T$ -matrix

$$T_{kk'}^{mm'}(z) \approx -\delta_{mm'} \frac{1}{N} n \tilde{I} / \left( n + n \tilde{I} \frac{1}{N} \sum_q \frac{1}{z - \epsilon_q} \right) \tag{19}$$



contains only one energy scale

$$n\bar{I} = nI\langle X_{mm} \rangle - [V^2 n / (z - \Delta E)]\langle X_{00} + X_{11} \rangle \approx I^*$$

i.e. again only the universal scale  $I^*$ . The last approximation  $n\bar{I} \approx I^*$  applies near the stable moment regime (which for  $I^* < 0$  would be called Kondo regime), where

$$0 \leq \langle X_{00} \rangle \ll \langle X_{mm} \rangle \approx 1/n$$

and for excitation energies  $|z| \ll |\Delta E|$ . For small  $z = \omega + i\delta$  and a featureless nearly symmetric band one obtains

$$T_{kk'}^{mm}(\omega + i\delta) \approx \frac{1}{N} \frac{-I^*}{n - i\pi I^* \mathcal{N}_F}$$

which gives rise to a moderate decrease of the DOS near the impurity at energies close to the Fermi level  $\epsilon_F = 0$ :

$$\mathcal{N}^c(\omega) = -\frac{1}{\pi} \frac{1}{N} \sum_{kk'} \text{Im} \langle \langle c_{km} | c_{k'm} \rangle \rangle (\omega + i\delta) \approx \frac{\mathcal{N}_F}{1 + (\pi \mathcal{N}_F I^*)^2}. \quad (20)$$

In arriving at the final result, the GF was first inserted in the form (10) with the energy-independent approximate  $T$ -matrix of above and then

$$\frac{1}{N} \sum_{\mathbf{q}} \frac{1}{\omega + i\delta - \epsilon_{\mathbf{q}}} \approx -i\pi \mathcal{N}_F$$

was used. In fact, spin-flip processes can be taken into account quite easily in this regime [23]. They contribute a term  $\langle X_{mm'} \rangle |_{m \neq m'}$  which is small and can be neglected in leading order. These considerations show that the AS resonance is not found in the ferromagnetic case due to the disappearance of many-body correlations; again only the scaling parameter  $I^*$  is involved. The new ferromagnetic correlations should lead only to a weak modification of the bare band DOS. Therefore equations (19) and (20) do not contain a structure like the small anti-resonance found recently in a numerical study of the Hamiltonian (1) [2]. A quantitative investigation is included in the next section.

### 3. Results and discussion

A standard for the following investigation of the scaling behaviour of the model (1) is set by the check of universality, which is known to hold for the Kondo problem [24]. Observable properties of the impurity should depend only on relative variables, measured in units of the dynamically generated energy scale  $k_B T_K$ , i.e.  $A(T) = A_0(T/T_K)$  where  $A_0$  is a universal function that is the adjunct to  $A$ , the specific heat, susceptibility or else. A particularly impressive demonstration of universality is furnished by a dynamical quantity such as the spectral density  $\mathcal{N}^{\text{loc}}(\omega)$ . In figure 1 equation (12) is calculated within NCA for the Anderson impurity at degeneracy  $n = 4$  [25] i.e. equation (1) with  $I = 0$ . Different values of the hybridization strength  $V$  have been used implying a variation of the indirect exchange coupling

$-J = V^2/\Delta E$ . The temperature was chosen at  $T = 0.6T_K$  in each case, with  $T_K$  according to equation (4) at  $\Delta^* = \Delta \equiv \pi N_F V^2$ . The calculations were made with a band of width  $2W$  and constant DOS  $N_F = 1/2W$ . The coordinates are scaled universally as  $\omega/k_B T_K$  and  $\pi \Delta N^{loc}$ . Shown is the low-energy region around the Fermi level. In spite of a sizable variation of  $\Delta$  by a factor 1.7 and a corresponding exponentially strong variation of the Kondo scale  $T_K$  up to a factor 25 all five curves nearly coincide, demonstrating perfect scaling of the AS resonance. The peak value is near the unitary limit  $\pi \Delta N^{loc}(\omega_{max}) = 1$ . It should be remarked, however, that this good approximation to ideal universal behaviour still reveals the presence of (virtual) charge fluctuations.

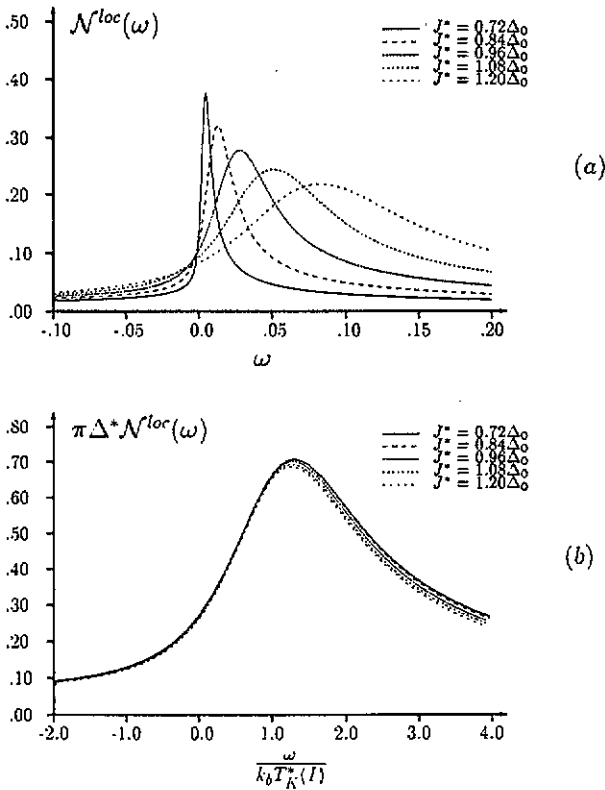


**Figure 1.** (a) Local density of states (DOS) in the vicinity of the Fermi level  $\epsilon_F = 0$  without direct exchange ( $I = 0$ ) against energy for different hybridization strength ( $J^* = J = V^2/|\Delta E|$ ); (b) the same data drawn with rescaled axes. Parameters:  $n = 4$ ,  $\Delta E = -5.3$ ,  $T = 0.6T_K$ . All energies are given in units of  $\Delta_0 = W/10$ , where  $W$  is the half band width.

A first test of our scaling hypothesis in the presence of both indirect exchange  $-J = V^2/\Delta E$  and direct (ferromagnetic) exchange  $I > 0$  is summarized in table 1. An increase of  $I$  from zero to  $0.4J$  at constant  $V$  and  $\Delta E$  causes a decrease of the one-particle scale  $\Delta^*$  from  $\Delta$  to  $0.6\Delta$  and a decrease of the effective many-body scale  $T_K^*$  from  $T_K = T_K^*(I = 0)$  to  $0.04T_K = T_K^*(I = 0.4J)$ . For larger values  $0.4J < I < J$  the numerical problem of resolving the tiny many-body effects could not be handled accurately enough. At  $I/J = 0.4$  the numerical accuracy is already

not very good due to slow convergence, which explains the deviations in the last row of table 1; essentially they are caused by the finite integral mesh. All quantities were calculated at constant universal temperature  $T/T_K^* = 0.6$ . The AS resonance peak ratio, i.e. the ratio of the maximum values  $\mathcal{N}^{\text{loc}}(\omega_{\text{max}})$  at the indicated value of  $I$  and at  $I = 0$ , should then simply equal the ratio  $\Delta/\Delta^*$  if perfect scaling would apply, the saturation value being  $\mathcal{N}^{\text{loc}}(\omega_{\text{max}}) = 1/\pi\Delta$  for the Anderson impurity at zero temperature. The position  $\omega_{\text{max}}$  of the AS resonance peak equals  $k_B T_K^*$  in the NCA for the Anderson impurity, independent of the degeneracy  $n$ . The corresponding mild violation of the DOS sum rule [13, 14] for  $n = 2$  is one of the shortcomings to be improved on by going beyond the NCA as indicated in section 2. One can nevertheless for small  $n$  also compare  $\omega_{\text{max}}(I = 0)$  to  $k_B T_K$  and the inverse AS resonance position ratio  $\omega_{\text{max}}(0)/\omega_{\text{max}}(I)$  to  $T_K/T_K^*$  for a check of the scaling hypothesis. Finally, the static susceptibility  $\chi_{\omega=0}(I = 0)$  at  $T = 0$  of the Anderson impurity equals  $1/(2\pi k_B T_K)$  [22, 24, 19] which can, together with the ratio  $\chi_0(I)/\chi_0(0)$ , be used to this end, too. With  $T_K \equiv T_K(I = 0) = 0.066\Delta$ ,  $\omega_{\text{max}}(I = 0) = 0.066\Delta$  and  $(\chi_0(0))^{-1} = 0.35\Delta$  the applicability of the NCA to Kondo's infrared problem is once again demonstrated. The reasonable agreement of the ratios compared in table 1 even for very small values of  $T_K^*$ , where numerical problems begin to arise, already points to the applicability of our scaling arguments. The deviations of up to 20% will be discussed later.

Table 1.

$I/J$	$\Delta/\Delta^*$	ASR peak ratio	$T_K/T_K^*$	Inverse ASR position ratio	$\chi_0(I)/\chi_0(0)$
0	1.00	1.00	1.00	1.00	1.00
0.1	1.11	1.21	1.63	1.72	1.66
0.2	1.25	1.47	3.00	3.28	3.16
0.3	1.43	1.78	6.51	7.57	7.34
0.4	1.67	2.08	18.2	25.0	21.8

A full justification of the scaling hypothesis comes from the study of the frequency dependence in spectral density  $\mathcal{N}^{\text{loc}}(\omega)$ , local  $T$ -matrix (14) and susceptibility  $\chi(\omega)$ . We show the corresponding universal functions (see above) for different values of  $I$  but identical value of  $T/T_K^*$  in figures 2, 3 and 4. Parts (a) respectively contain selected raw data, whereas the plots in parts (b) with scaled coordinate axes (as indicated above) should reveal that these data represent essentially the same universal curve. It is quite obvious that the simple scaling procedure, i.e. fixing of the universal temperature parameter  $T/T_K^*$  and gauging the energy axis  $\omega \rightarrow \omega/(k_B T_K^*)$  and likewise the ordinate in units appropriate for the respective observable

$$\mathcal{N}^{\text{loc}} \rightarrow \pi \Delta^* \mathcal{N}^{\text{loc}} \quad -\text{Im } T_{\text{loc}} \rightarrow -\pi \mathcal{N}_F \text{Im } T_{\text{loc}} \quad \text{Im } \chi \rightarrow k_B T_K^* \text{Im } \chi$$

essentially removes the large deviations between the curves at different values of  $I$  near the Fermi level. Remaining discrepancies are less by an order of magnitude and again amount up to 20% [7]. Here, too, the curves for  $I = 0.4J$  have to be treated with care for reasons mentioned above. The theoretical saturation peak value for the scaled quantities  $\pi \Delta^* \mathcal{N}^{\text{loc}}$ ,  $-\pi \mathcal{N}_F \text{Im } T_{\text{loc}}$  and  $2\pi k_B T_K^* \text{Re } \chi(0)$  would be one at  $T = 0$ . A discussion of these discrepancies will be taken up below. The approximate,

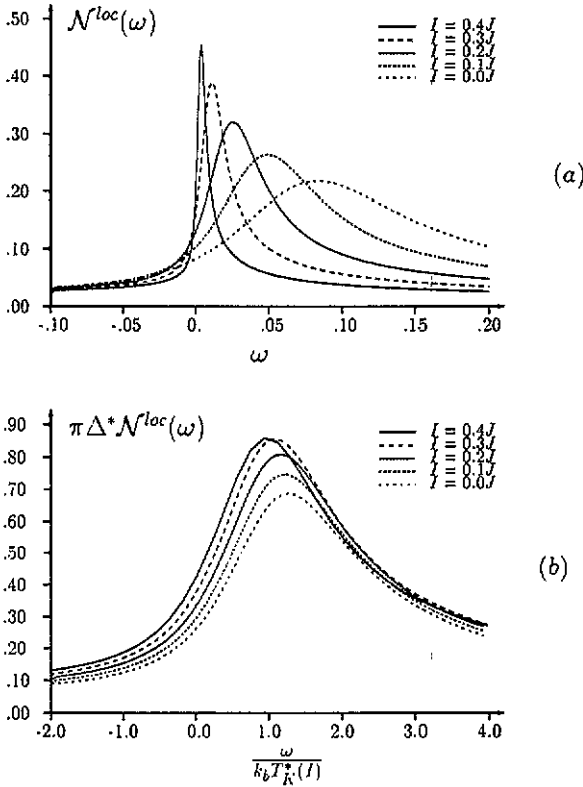


**Figure 2.** (a) Local density of state in the vicinity of the Fermi level  $\epsilon_F = 0$  against energy for constant hybridization strength ( $J = V^2/|\Delta E| = 1.2\Delta_0$ ) and increasing direct exchange  $I$ ; (b) the same data drawn with rescaled axes. Parameters as in figure 1.

but nevertheless clear, applicability of universal functions taken from the Anderson model (1) with  $I = 0$  to the set of dynamical data at values  $0 < I/J < 1$  is taken as a strong justification for the scaling hypothesis.

Considering the ferromagnetic regime  $I^* > 0$ , figure 5(a) shows the imaginary part of the  $T$ -matrix over a large energy region at  $I^* = 0.5J$  and in addition the corresponding curve calculated from the suggested theoretical scaling behaviour equation (19) due to one-particle scattering only. Although some deviations are found, one may conclude that: (i) most features of the NCA and the theoretical  $T$ -matrix approximation agree at least qualitatively, i.e. a broad peak near the original resonance, a widely smeared out maximum above the Fermi level and some band edge effects around  $\omega = -10$ ; (ii) the absence of pronounced many-body effects at  $\omega = 0$ . Apparently the band edge effect at the lower edge is more drastic in the NCA calculation whereas the analytical formula only furnishes a wide tail. We attribute this feature, as well as the small dip at  $\omega = 0$ , to well known shortcomings of this approximation [9, 10]. The scaling hypothesis for our model (1) treated in extended NCA in the ferromagnetic regime is tested in figure 5(b). Apparently, the data for different values of  $I^*$  between  $0.5J$  and  $1.0J$  can, by simply dividing  $\text{Im } T$  by  $I^*$ , already be mapped onto an universal curve around and above the Fermi level. All together the agreement seems to be quite reasonable, proving not only the absence

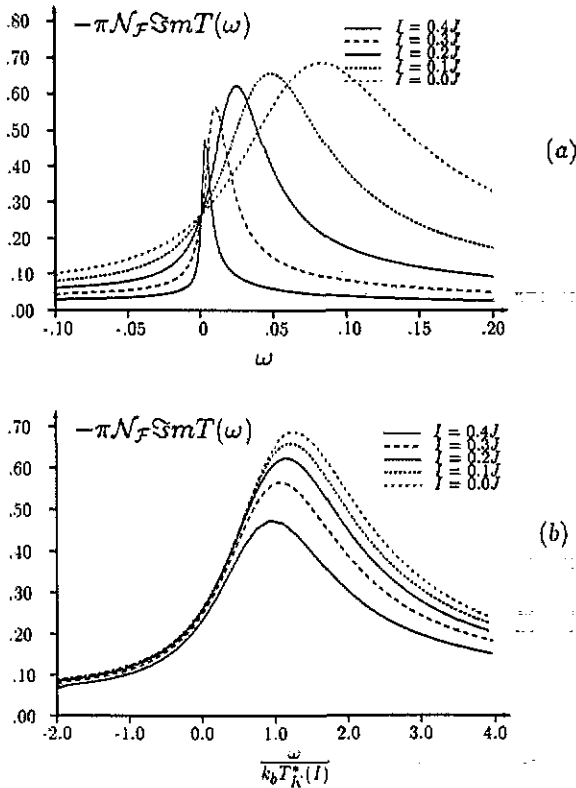


**Figure 3.** (a) Imaginary part of the local  $T$ -matrix in the vicinity of the Fermi level  $\epsilon_{\mathcal{F}} = 0$  against energy for constant hybridization strength ( $J = V^2/|\Delta E| = 1.2\Delta_0$ ) and increasing direct exchange  $I$ ; (b) the same data drawn with rescaled axes. Parameters as in figure 1.

of many-body correlations as argued before but also the existence of only one scaling parameter  $I^*$  which rules the physics of the impurity in this regime in the sense of equations (19) and (20). The analytical approximation on the other hand can also not be expected to be quantitatively correct. Spin-flip processes certainly contribute although no infrared catastrophe is generated here. In order to keep these at a minimum we have chosen  $n = 2$  in figure 5.

As additional evidence for the picture developed we present the local DOS for the ferromagnetic regime in figure 6. Again qualitative agreement between the NCA and an analytic approximation [26] consistent with the  $T$ -matrix (19) can be stated: the absence of many-body effects near the Fermi level is obvious. Furthermore figure 7 contains a calculation of the  $T$ -matrix of the antiferromagnetic  $s$ - $d$  model, i.e. equation (1) at  $V = 0$  and  $I < 0$ , and in figure 8 the free energy connected with the impurity as a function of  $T_K^*$  in the presence of both exchange mechanisms is plotted. Whereas one can learn from the former about the universal effect of an antiferromagnetic exchange, direct or indirect, the latter reveals the effective  $T_K^*$  as the universal measure of the spin-compensation energy. The  $T$ -matrix in figure 7 resembles closely the AS resonance shown in figure 1 although no hybridization is present here. The band electrons apparently are scattered via the direct interaction  $I < 0$  as if a fictitious hybridization  $V^*$  with a fictitious local level  $\Delta E^* < 0$

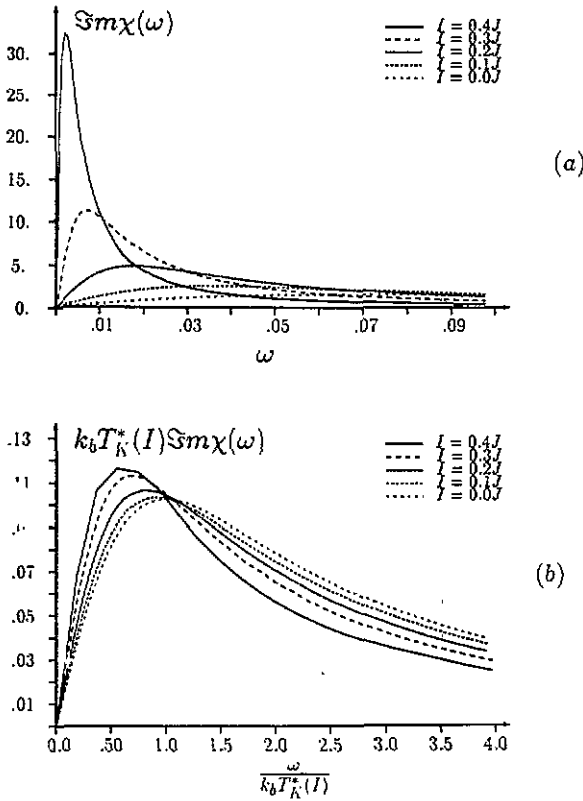


**Figure 4.** (a) Imaginary part of the local magnetic susceptibility in natural units in the vicinity of the Fermi level  $\epsilon_F = 0$  against energy for constant hybridization strength ( $J = V^2/|\Delta E| = 1.2\Delta_0$ ) and increasing direct exchange  $I$ ; (b) the same data drawn with rescaled axes. Parameters as in figure 1.

were at work, fulfilling  $I = V^{*2}/\Delta E^* < 0$ . This picture agrees well with the philosophy underlying the Schrieffer–Wolff transformation [4]. It should, however, be stated that the NCA works rather poorly for the s–d model without hybridization in a quantitative sense. The size of the resonance generally comes out too large, i.e. about a factor of 1.5 in figure 7. The enhancement is caused by the denominators  $1 - I\chi(z)$  in equation (16) which tend to zero near  $\omega = 0$  for antiferromagnetic  $-I \approx J$  at  $T < T_K^*$ . This difficulty is connected with the deviations found above in the ferromagnetic regime, where  $I$  was already larger than the indirect exchange  $J$ . The free energy  $F_{loc}$  (figure 8) may be thought of as containing two pieces: (i) the unperturbed  $F_{ion} = \Delta E_m$  (strictly one electron present and  $k_B T \ll |\Delta E|$ ) of the free ion, and (ii) a part  $\Delta F$  due to the interaction with the band states, which may at  $T < T_K^*$  in the many-body regime be characterized as spin-compensation energy. For the pure Kondo problem this last part essentially is again  $k_B T_K$ , whereas in the presence of charge fluctuations, i.e.  $V > 0$  and  $J > 0$ , an additional contribution due to scattering of band electrons in the one-particle resonance near  $\Delta E$  arises. The variation of  $\Delta F = F_{loc} - F_{ion}$  with a ferromagnetic direct exchange contribution  $I$  at fixed indirect exchange  $-J$  in figure 8(a) reveals a negative contribution at  $I = 0$ , which we assign to the spin-compensation plus resonant-scattering energy of an Anderson impurity and, when  $T_K^*(I)$  is chosen for the abscissa, a near-linear

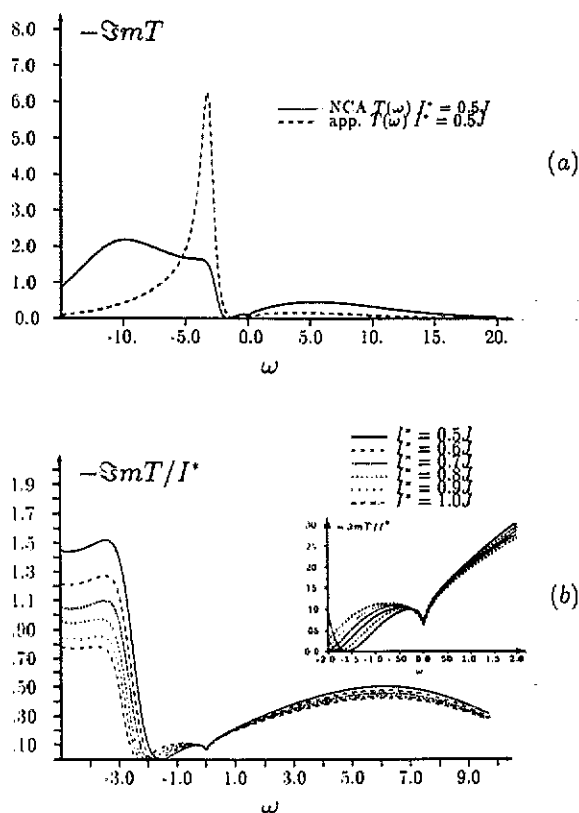


Figure 5. (a) Imaginary part of the local NCA  $T$ -matrix (16) and analytical  $T$ -matrix (19) against energy in the ferromagnetic regime for  $I^* = 0.5J$ . (b) Extended NCA calculation for a series of values  $I^* = 0.5, \dots, 1.0J$ , normalized to  $I^*$  in order to show scaling. Parameters:  $n = 2$ ,  $\Delta E = -3\Delta_0$ ,  $\beta = 62.41/\Delta_0$ .

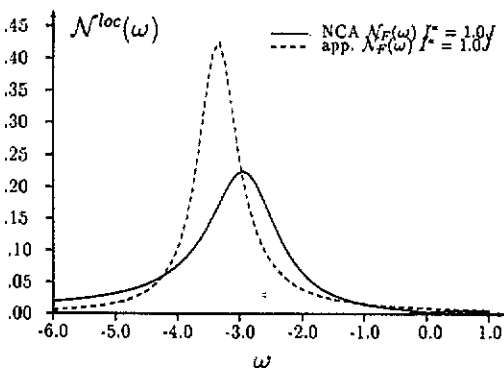


Figure 6. Local DOS in NCA and analytic approximation for  $I^* = J$  in the ferromagnetic regime. Parameters as in figure 5.

decrease with increasing  $T_K^*$ . This indicates essentially an increase in the energy gained by local spin compensation due to a reduction of  $I$ . Note that  $T_K^*$  increases with decreasing  $0 < I < J$  and vice versa. For antiferromagnetic direct exchange

$I < 0$  an analogous effect is found, i.e.  $\Delta F$  again decreases nearly linearly with increasing  $T_K^*$ , the latter being now a direct measure of the growing total value  $-I$ . In the ferromagnetic regime the leading contribution to  $\Delta F$  is expected to depend linearly on  $I^{*2}$  as can be seen in figure 8(b). This behaviour of the free energy implies scaling of thermodynamic quantities, such as the static susceptibility which has been discussed above, see e.g. table 1. The connection may be elaborated on by additional examples such as the specific heat which underline our point of view. Therefore scaling, as found for the Hamiltonian (1) with two exchange interaction mechanisms, encompasses the universality of the Kondo problem, is independent of the formulation via an Anderson or an s-d model and pertains to thermodynamic and dynamical quantities.

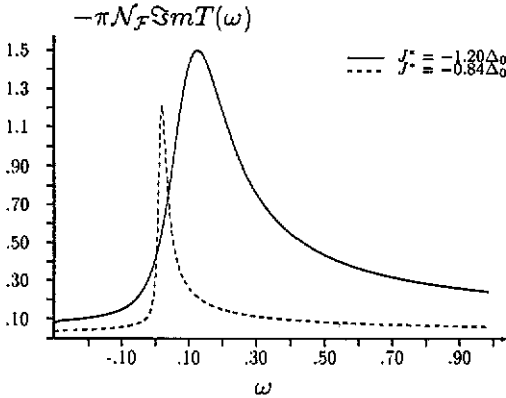
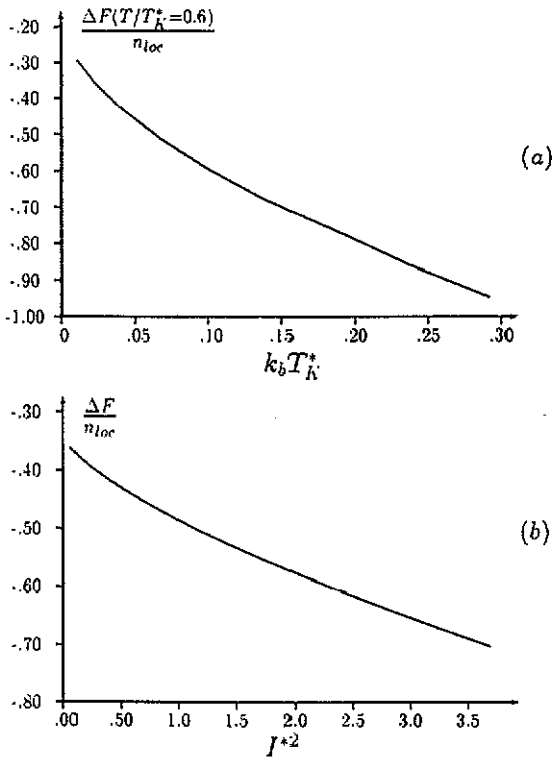


Figure 7. Imaginary part of the local  $T$ -matrix against energy for  $V = 0$  and anti-ferromagnetic  $I$ ; ( $J = 1.2\Delta_0$ ) at  $T = T_K^*$ . Parameters as in figure 1.

#### 4. Conclusion

A general agreement of all the results presented with the expectations raised by the scaling hypothesis formulated in the first section has been found with quantitative deviations of up to ten per cent, in rare cases somewhat more. Apart from peculiarities connected with specific observables, such as in case of numerical prefactors for the dynamic energy scale  $k_B T_K$  [24], five general sources of errors can be named: (i) The NCA itself as an approximation, which e.g. generates a small pathology in spectra near the Fermi level [9, 27], causing some deviations at small excitations energies and in particular numerical problems at  $T \ll T_K^*$ . (ii) Stability problems of numerical procedures for very low Kondo temperature  $k_B T_K^* \ll \Delta$ , where structures near the Fermi level become very sharp on the natural one-particle scale  $\Delta$  of the problem. (iii) The need for a non-zero temperature  $T \geq 0.6 T_K^*$  in all calculations, at which the theoretically predicted saturation values, i.e.  $\omega_{max} = k_B T_K^*$  for  $T = 0$ , have not yet been reached. (Closed analytical formulas for non-zero temperature are generally not available.) (iv) The presence of charge fluctuations at non-zero hybridization which contribute to all observables and for the chosen and convenient set of parameters typically give up to ten percent corrections to the Schrieffer-Wolff mapping, even in view of its extended validity [8]. (v) In additional numerical studies





**Figure 8.** Free energy difference  $\Delta F$  for constant hybridization strength ( $J = V^2/|\Delta E| = 1.2\Delta_0$ ) and increasing direct exchange (a) in the antiferromagnetic regime against the Kondo temperature at constant temperature ratio  $T/T_K^* = 0.6$ . (b) in ferromagnetic regime against  $I^{*2}$ . Parameters as in figure 1.

non-universal features were seen, such as a dependence of the non-exponential part of the ‘true’ dynamical scale  $T_K^*$  on bandstructure. Note that there is a possible explicit impact of  $I$  onto the prefactor of the Kondo temperature (4) as proposed in [7]. Altogether the deviations observed are of the expected size and can be explained by these five sources essentially. With regard to the overall picture, a failure of an effective Schrieffer–Wolff transformation would indicate a more complicated interplay of hybridization and direct exchange. The contribution (4) also sets the limits of our scaling picture. Real charge fluctuations, on the other hand, being important in the intermediate-valence regime [28], reduce the importance of any type of exchange interaction due to a destabilization of the local moments.

In conclusion, we have shown how the competition of two different exchange mechanisms in the presence of strong local correlations can be understood via a simple scaling hypothesis. Evidence presented includes thermodynamic and dynamical observables and encompasses the spin-compensated many-body regime as well as a ferromagnetic regime, in which the impurity can essentially be described in one-particle terms. In particular, no signs of additional correlation effects were found, contrary to earlier suggestions [1, 2]. It will, however, certainly be interesting to extend the present study to the lattice case, where e.g. non-local magnetic correlations, cooperative magnetism and corresponding phase transitions might be encountered. The extension beyond NCA, as outlined in section 2, will certainly improve the ac-

curacy of our results and might be essential for a treatment of the Hamiltonian (1), properly extended to the lattice. From the point of view of an extended bandstructure calculation, with particular routines implemented to handle strong correlations as might be necessary for certain transition metal compounds [29], the present study could be very useful. It demonstrates that certain Coulomb-matrix elements may well be taken into account via a few effective parameters. We plan to extend this investigation to other types of matrix elements such as the Falicov–Kimball term.

## Acknowledgments

Useful conversations with R Freytag and Professor J Keller are gratefully acknowledged. One of us (QQ) would like to thank Professor H Keiter for fruitful discussions. This work was performed within the research programme of SFB 252 'Elektronisch hochkorrelierte metallische Materialien', Darmstadt, Frankfurt/Main, Mainz, Federal Republic of Germany.

## References

- [1] Keller J, Bauer A and Freytag R 1991 *Z. Phys. B* **83** 372
- [2] Freitag R and Keller J 1991 *Z. Phys. B* **85** 87
- [3] Grüner G and Zawadowski A 1974 *Rep. Prog. Phys.* **37** 1497
- [4] Schrieffer J R and Wolff P A 1966 *Phys. Rev.* **149** 491  
Mühschlegel B 1968 *Z. Phys.* **208** 94
- [5] Grewe N and Keiter H 1981 *Phys. Rev. B* **24** 4420  
Keiter H and Morandi G 1984 *Phys. Rep.* **109** 227
- [6] Wilson K G 1975 *Rev. Mod. Phys.* **47** 733
- [7] The study presented here is based on a straight forward extension (4) of the analytical Kondo temperature. Interestingly, with a different prefactor
 
$$T_K^{\text{test}} = W \left( \frac{N_F}{\Delta} \left( J\Delta \cdot \frac{|\Delta E|}{W} - I(\Delta - \Delta^*) \right) \right)^{1/n} \exp \left[ -\frac{\pi |\Delta E|}{n\Delta^*} \right]$$
 for  $V \neq 0$ , suggested for a mixture of  $T_K^*$  and the  $T_K^{\text{CS}}$  [19], and a Gaussian band DOS perfect scaling was found for  $\chi(\omega)$  and  $T(\omega)$  but not for the local DOS. Although the scaling picture may improve by such more elaborate considerations we do not want to overemphasize here the detailed quantitative aspects of the scaling.
- [8] Keiter H and Kimball J C 1971 *Int. J. Magn.* **1** 233
- [9] Grewe N 1983 *Z. Phys. B* **53** 271  
Kuramoto Y and Hüller-Hartmann E 1985 *J. Magn. Mater.* **52** 122  
Bickers N E, Cox D L and Wilkins J W 1987 *Phys. Rev. B* **36** 2036
- [10] Grewe N 1984 *Solid State Commun.* **50** 19  
Grewe N, Pruschke Th and Keiter H 1988 *Z. Phys. B* **71** 75
- [11] Grewe N and Pruschke Th 1990 *Solid State Commun.* **67** 205  
Pruschke Th 1990 *Z. Phys. B* **81** 319
- [12] Pruschke Th and Grewe N 1989 *Z. Phys. B* **74** 439
- [13] Shiba H 1975 *Prog. Theor. Phys.* **54** 967  
Yamada K 1975 *Prog. Theor. Phys.* **54** 67
- [14] Anders F B, Grewe N and Lorek A 1991 *Z. Phys. B* **83** 75
- [15] Kuramoto Y and Kojima H 1984 *Z. Phys. B* **57** 95
- [16] Qin Qi, Grewe N and Anders F B 1992 *DPG Spring meeting (Regensburg, Federal Republic of Germany)* paper presented
- [17] Baym G 1962 *Phys. Rev.* **217** 1391
- [18] Anders F B, Grewe N and Qin Qi to be published

- [19] Bickers N E 1987 *Rev. Mod. Phys.* **59** 845  
 [20] Menge B and Müller-Hartmann E 1988 *Z. Phys.* **B 73** 225  
 Keiter H and Qin Qi 1990 *Z. Phys.* **B 79** 397  
 [21] Haensch R, Keitel G, Schreiber P, Sonntag B and Kunz C 1969 *Phys. Rev. Lett.* **23** 528; 1970 *Phys. Status Solidi a* **2** 85  
 Nozières P and de Dominicis C T 1969 *Phys. Rev.* **178** 1097  
 [22] Krishna-murthy H R, Wilkins J W and Wilson K G 1980 *Phys. Rev.* **B 21** 1003; 1980 *Phys. Rev.* **21** 1044  
 [23] The most detailed result for the  $T$ -matrix

$$T^{mm'}(z) = -(1/N)(I^*/(1 + I^*D(z)/n)^2 + \langle X_{nd} \rangle (I^*D(z))^2 [1 - 2/n + (n-1)\langle X_{nd} \rangle]) \\ * \{ \delta_{mm'} [(1 + I^*D(z)/n)/n + I^*D(z)\langle X_{nd} \rangle (1 - 2/n + (n-1)\langle X_{nd} \rangle)] \\ + (1 - \delta_{mm'}) \langle X_{nd} \rangle \}$$

contains spin-flip processes resembled in the expectation value

$$\langle X_{nd} \rangle := \langle X_{mm'} \rangle |_{m \neq m'} \left( D(z) = \frac{1}{N} \sum_k \frac{1}{z - \epsilon_k} \right).$$

- [24] Tselik A M and Wiegmann P B 1983 *Adv. Phys.* **32** 453  
 [25] Due to the difficult numerical procedures sometimes  $n \geq 4$  had to be chosen in order to achieve convergence in the temperature regime  $T < T_K^*$  for small antiferromagnetic  $I^*$ .  
 [26] The suggested form of the local GF

$$\langle \langle X_{0m} | X_{m0} \rangle \rangle (z) = \frac{\langle X_{mm} \rangle + \langle X_{00} \rangle}{z - \Delta E - E_{\text{tad}} - V^2 (\langle X_{mm} \rangle + \langle X_{00} \rangle D(z)) / (1 + I \langle X_{mm} \rangle D(z))}$$

has been obtained with the equation of motion technique. The tadpole contribution  $E_{\text{tad}}$  is thought to be absorbed into  $\Delta E$  in all calculations.

- [27] Müller-Hartmann E 1984 *Z. Phys.* **B 57** 281  
 [28] Jefferson J H and Stevens K W H 1978 *J. Phys. C: Solid State Phys.* **11** 3919  
 Hewson 1979 *J. Magn. Mater.* **12** 83  
 Lawrence J M, Riseborough P S and Parks R D 1981 *Rep. Prog. Phys.* **44** 1  
 [29] Sticht J, d'Ambrumenil N and Kübler J 1986 *Z. Phys.* **B 65** 149